Soil Dynamics and Earthquake Engineering 36 (2012) 32–37

Contents lists available at SciVerse ScienceDirect

Soil Dynamics and Earthquake Engineering

journal homepage: www.elsevier.com/locate/soildyn

The uncertainties of a *Pd3–PGV* onsite earthquake early warning system

Jui-Pin Wang [a,*], Yih-Min Wu [b], Ting-Li Lin [c], Logan Brant [d]

[a] Department of Civil & Environmental Engineering, The Hong Kong University of Science and Technology, Clear Water Bay, Kowloon, Hong Kong
[b] Department of Geosciences, National Taiwan University, Taipei, Taiwan
[c] Department of Earth Sciences, National Cheng Kung University, Tainan, Taiwan
[d] Department of Civil Engineering and Engineering Mechanics, Columbia University, New York City, USA

ARTICLE INFO

Article history:
Received 16 March 2011
Received in revised form
30 August 2011
Accepted 29 December 2011
Available online 31 January 2012

ABSTRACT

Earthquake early warning systems have been developed to help minimize the loss of life and other damages resulting from catastrophic earthquakes. In the past several decades, these systems have evolved to function using a variety of methodologies. This study introduces an onsite system developed from a correlation between the precursor measurement (*Pd3*) and the peak ground acceleration (*PGV*) from 780 historical earthquake events recorded in Taiwan, Japan and South California. The study analyzes and integrates the uncertainty of the onsite system, establishing the statistical relationship between the *PGV* forecast, the *Pd3* precursor, and the exceedance probability (P_E). A method is presented for forecasting the *PGV* by scaling the *Pd3*. Furthermore, this study also suggests a decision-making model to determine whether or not the early warning notification should be issued, based on factors such as the uncertainty of the early warning system, the magnitude of the precursor, and warning recipient characteristics.

1. Introduction

Catastrophic earthquakes can be devastating to human populations, as demonstrated by the 2010 Haiti earthquake with a reported magnitude of 7.0 and which resulted in an estimated death toll of more than 150,000. To help reduce the dreadful consequences of catastrophic earthquakes, the scientific community is working on better understanding the factors creating these disasters and on what can be done to mitigate future damage. Such work requires learning more about the mechanisms that generate earthquakes, improving our abilities to predict earthquakes, and expanding the use of hazard mitigation methods, including the development and implementation of earthquake early warning systems.

This study examines the uncertainty of one specific onsite model that uses the relationship between the first three second peak displacement (*Pd3*) as a precursors to aid in the prediction of the peak ground velocity (*PGV*) [1]. The paper includes an overview of the early warning system and provides a statistical evaluation to quantify the uncertainty of the model. A risk-based, decision-making model is also described as part of the onsite early warning system. The model considers factors such as the uncertainty of the early warning systems, the magnitude of precursors, and the characteristics of warning recipients.

2. Earthquake early warning systems

In the past several decades, earthquake early warning systems have been proposed based on a variety of different methodologies [1–8]. The idea behind these systems is to provide timely alerts ahead of the arrival of an earthquake's destructive peak ground motion. Earthquake early warning systems are believed to provide a practical and effective tool to assist with seismic risk mitigation [9,10].

There are two types of earthquake early warning systems: regional systems and onsite systems. Regional systems collect and analyze seismic data from multiple stations to provide early warnings to distant sites. In contrast, onsite systems use precursor measurement from the early part of the earthquake ground motion to provide information for that same specific site. Onsite systems are generally faster, but less accurate than the regional systems [4,5].

All earthquake early warning models contain uncertainties due to the natural randomness of earthquakes, influenced by the factors such as seismic-wave propagations, site characteristics, and other unpredictable variables. Discussions of the uncertainties of the earthquake early warning model predictions have been relatively limited, particularly for onsite systems. Iervolino et al. [11–14] provided a study of the uncertainty of regional early warning models and developed real-time probabilistic seismic hazard

* Corresponding author. Tel.: +852 2358 8482; fax: +852 2358 1534.
E-mail address: jpwang@ust.hk (J.-P. Wang).

0267-7261/$ - see front matter © 2012 Elsevier Ltd. All rights reserved.
doi:10.1016/j.soildyn.2011.12.005

analysis (RTPSHA). A similar framework was applied in other real-time forecasts, such as peak ground acceleration, response spectra, and expected loss, for a potential catastrophic event [15].

3. *Pd3–PGV* early warning system

3.1. Onsite Pd3–PGV model

This study illustrates model uncertainty and its impact on early warning forecasts for a specific onsite early warning system that was developed based on a total of 780 historical waveforms gathered from Taiwan, Japan and South California. Fig. 1 shows the distribution of the 780 pairs of *Pd3* and *PGV*. A strong correlation was observed between the two variables. The simple linear regression model (SLRM) describes this relationship as follows:

$$\log(PGV) = 1.52 + 0.81\log(Pd3) \tag{1.1}$$

The equation has a correlation coefficient (r) of 0.87 and a standard deviation (s) of 0.32. The intrinsically linear relationship between *Pd3* and *PGV* is

$$PGV = 32.98Pd3^{0.81} \tag{1.2}$$

3.2. Deterministic application of the model

In the model the *Pd3* serves as a precursor used to aid in predicting *PGV* that will follow. With a deterministic evaluation the model uncertainty is not factored in the forecast, although the standard deviation may be calculated. Using this approach the estimate is very unlikely to be identical to the actual observation. The estimate has a 50–50 probability of either being greater or less than the actual observation.

4. Linear regression

Linear regression analyses are widely used in correlation analyses and are available in most statistical computer packages. The accessibility of this method causes it to sometimes be applied incorrectly for the interpretation of data. Linear regression is only appropriate when the residual is normally distributed. For data where this is not the case other types of correlations, such as polynomial functions, might be better suited.

Fig. 2 shows the distribution of the 780 standardized residuals (e_i^*) of the onsite system. The expression of e_i^* is as follows:

$$e_i^* = \frac{y_i - \hat{y}_i}{\sigma_{Y_i-\hat{Y}_i}} \tag{2.1}$$

where y_i and $\hat{y}_i$ denote the ith observation and ith estimate associated with the dependent variable Y. $\sigma_{Y_i-\hat{Y}_i}$ is the standard deviation of $Y_i-\hat{Y}_i$, and is as follows:

$$\sigma_{Y_i-\hat{Y}_i} = s\sqrt{1-\frac{1}{n}-\frac{(x_i-\bar{x})^2}{\sum_{i=1}^{n}(x_i-\bar{x})^2}} \tag{2.2}$$

where x_i and $\bar{x}$ denote the ith observation and the mean value associated with independent variable X. For this study the dependent variable Y and the independent variable X are $\log(PGV)$ and $\log(Pd3)$, respectively.

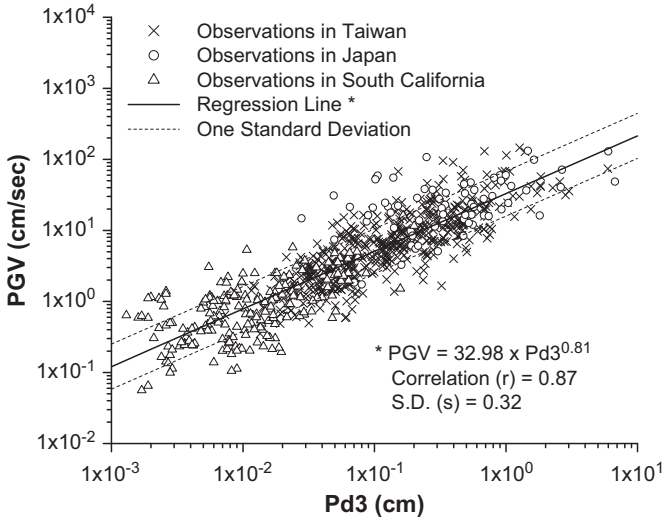

Fig. 1. Seven hundred and eighty observations of *Pd3* and *PGV* collected from Taiwan, Japan and South California. It appears an intrinsically linear relationship as: $PGV = 32.98 \times Pd3^{0.81}$. The correlation coefficient (r) and standard deviation (s) are 0.87 and 0.32, respectively.

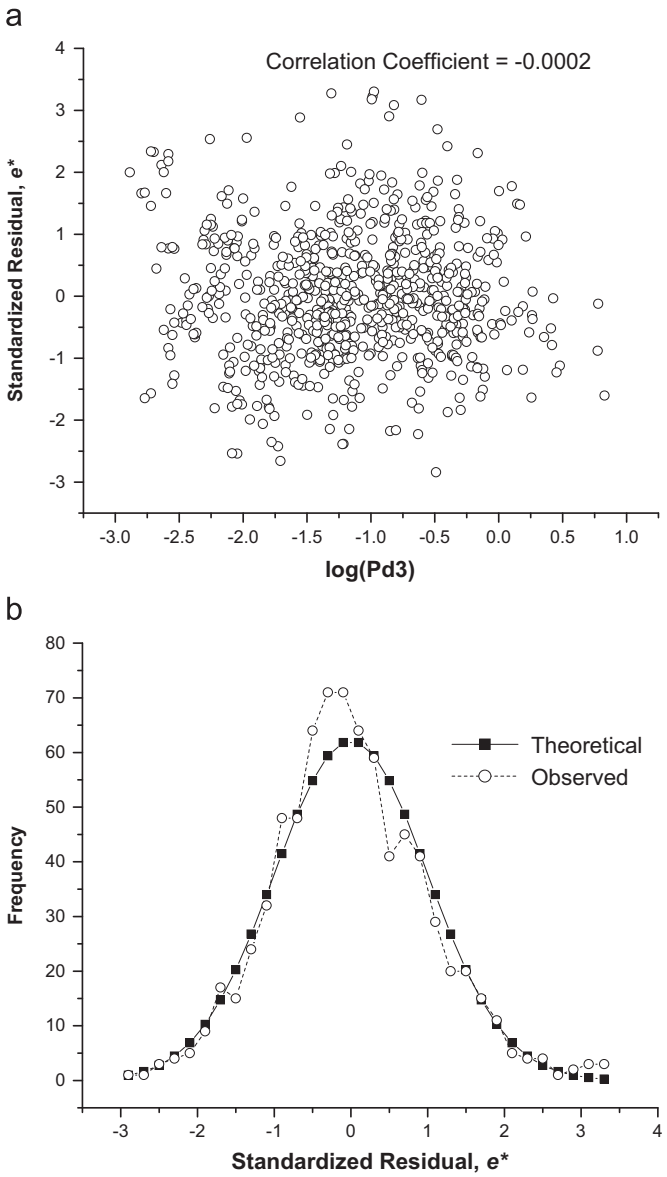

Fig. 2. Distribution of 780 standardized residuals: (a) standardized residuals are independent of $\log(Pd3)$ and (b) standardized residuals can be presented acceptably by a standard normal distribution.

In Fig. 2(a) $e_i^*$was found to be independent of log(*Pd3*) with the correlation coefficient close to zero ($=-0.0002$). Fig. 2(b) shows a good agreement between the observed distribution and the standard normal distribution. It suggests that the linear regression model is appropriate, since the model requirements are fulfilled.

5. Estimated *PGV* and its exceedance probability, P_E

5.1. Exceedance probability, P_E

Based on regression analysis the normalized forecast for Y at a given x^* follows a t-distribution associated with $n-2$ degrees of freedom, where n is the number of observation pairs

$$T=\frac{Y-\hat{y}_{x^*}}{S_{x^*}} \tag{3}$$

where $\hat{y}_{x^*}$ and $S_x{}^*$ are constants calculated from observations (see Appendix I). For a given forecast y^*, P_E is as follows:

$$P_E(y^*|x^*)=\mathbf{P}(Y>y^*|x^*)=1-\mathbf{P}(Y\le y^*|x^*)=1-F_{T,n-2}\left(\frac{y^*-\hat{y}_{x^*}}{S_{x^*}}\right) \tag{4}$$

where $F_{T,n-2}$ denotes the cumulative probability function of a t variate associated with $n-2$ degrees of freedom. In other words, $P_E(y^*|x^*)$ represents the exceedance probability for a given forecast y^* and precursor x^*. A *PGV* forecast at a given P_E and x^* can also be back-calculated (see Appendix II).

5.2. Exceedance probability for the onsite early warning system

Fig. 3 shows the relationships between the *Pd3* and the P_E considering five *PGV* forecasts; 1, 5, 10, 50 and 100 cm/s. With an observed *Pd3* of 0.1 cm, the exceedance probabilities are 98%, 50%, 18%, 0.09% and 0.0025%, respectively, for the five PGV values used in Fig. 3, providing a negative correlation with the *PGV* forecasts. Fig. 4 shows the *Pd3–PGV* relationships associated with five exceedance probabilities: 50%, 10%, 5%, 1% and 0.1%. When the observed *Pd3* was equal to 0.1 cm, the *PGV* forecasts were 5.08, 12.97, 16.92, 27.89, and 48.93 cm/s, respectively, for the five exceedance probabilities used in Fig. 4. In contrast, the *PGV* forecasts show a positive correlation with the exceedance probability for each given *Pd3*. Notice that the 50% exceedance probability curve is equal to the regression line (Eq. (1.2)).

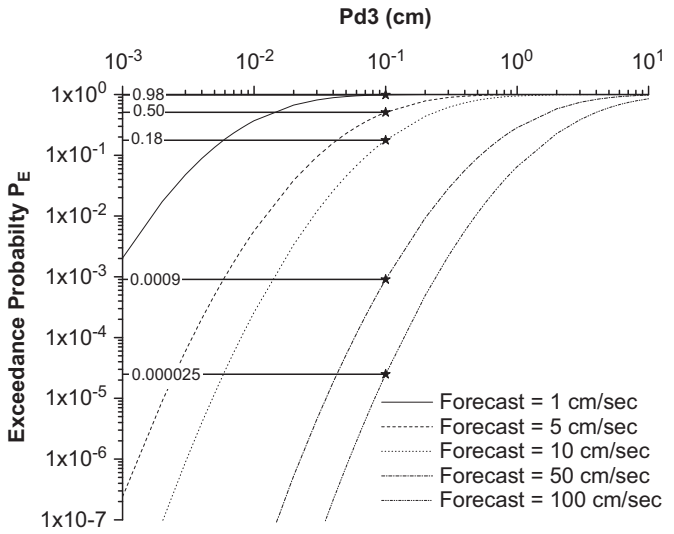

Fig. 3. Relationships between *Pd3* and exceedance probability for *PGV* forecasts of 1, 5, 10, 50, and 100 cm/s. When an observed *Pd3* is 0.1 cm, the respective exceedance probabilities are 98%, 50%, 18%, 0.09% and 0.0025%.

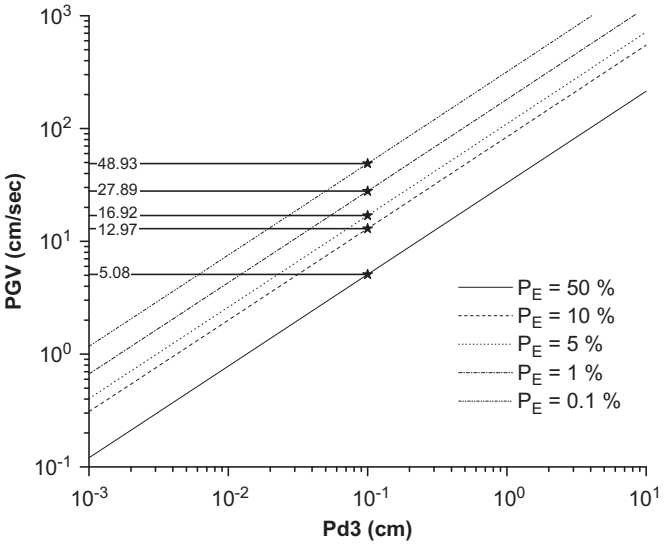

Fig. 4. Relationships between *Pd3* and *PGV* for exceedance probabilities of 0.1%, 1%, 5%, 10% and 50%. When an observed *Pd3* is 0.1 cm, the respective PGV forecasts are 5.08, 12.97, 16.92, 27.89 and 48.93 cm/s.

6. Generalized *PGV* forecast

This section develops generalized equations to conveniently forecast an approximate, but conservative, *PGA* from a *Pd3* and a given exceedance probability. We define R as the ratio $PGV_p{}^*/PGV_{50\%}$, where $PGV_p{}^*$ and $PGV_{50\%}$ represent the *PGV* forecasts associated with exceedance probabilities equal to p^* and 50%, respectively. In Fig. 4, R is equal to 3.33 (from 16.92/5.08), when p^* is 5% and *Pd3* is 0.1 cm. R is a function of P_E and *Pd3*.

Fig. 5 shows the distributions of R associated with four exceedance probabilities for given *Pd3* values ranging from 0.001 to 10 cm. R_{max} was observed at the lowest *Pd3*. In contrast, R_{min} corresponds to a *Pd3* between 0.1 and 1 cm. The variation of R was found to be insignificant, with a ratio of $R_{max}-R_{min}/R_{max}$ less than 1.5%. Fig. 6 shows the distribution of R_{max} for the onsite early warning system. For exceedance probabilities equal to 0.1%, 1%, 5%, 10%, and 50%, the corresponding R_{max} values are 9.75, 5.54, 3.36, 2.57 and 1.0, respectively. A slightly non-linear relationship and negative correlation between R_{max} and log(*Pd3*) was observed. Fig. 6 shows that R_{max} becomes a function of the exceedance probability and takes the form of $R_{max}=g(p^*)$.

$R_{max}\times PGV_{50\%}$ can be used to approximate $R\times PGV_{50\%}$, because $R_{max}\cong R$, and the former must be larger than the latter. This study introduces $R_{max}\times PGV_{50\%}$ to be a generalized *PGV* forecast (PGV_G), which is an approximate, but slightly more conservative prediction compared to $R\times PGV_{50\%}$. For the onsite system the general equation is as follows:

$$PGV_{G,p^*}=R_{max}\times PGV_{50\%}=g(p^*)32.98Pd3^{0.81} \tag{5}$$

where R_{max} can be found graphically from Fig. 6. With the substitution of R_{max} into Eq. (5) the generalized *PGV* associated with 0.1%, 1%, 5%, 10%, and 50% exceedance probabilities are as follows:

$$\begin{aligned}
PGV_{G,p^*=0.1\%}&=9.7\times 32.98Pd3^{0.81}=320Pd3^{0.81}\\
PGV_{G,p^*=1\%}&=5.5\times 32.98Pd3^{0.81}=181.4Pd3^{0.81}\\
PGV_{G,p^*=5\%}&=3.36\times 32.98Pd3^{0.81}=110.8Pd3^{0.81}\\
PGV_{G,p^*=10\%}&=2.55\times 32.98Pd3^{0.81}=84Pd3^{0.81}\\
PGV_{G,p^*=50\%}&=1\times 32.98Pd3^{0.81}=32.98Pd3^{0.81}
\end{aligned} \tag{6}$$

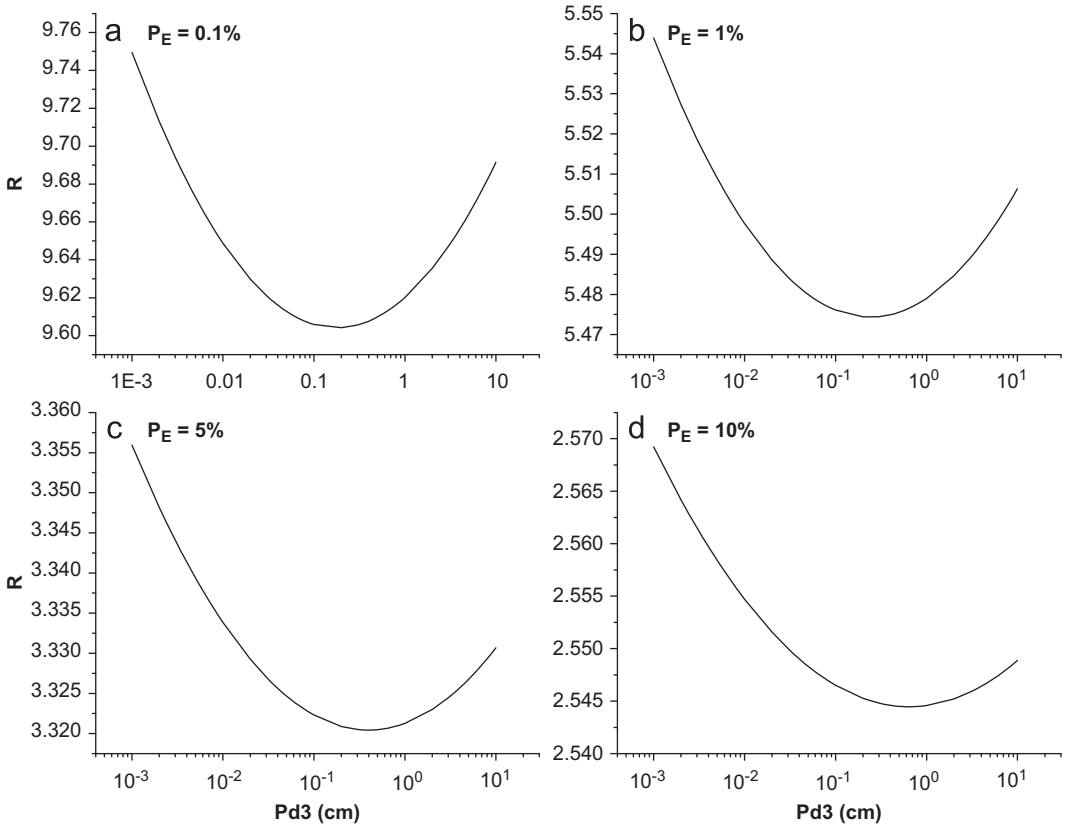

Fig. 5. Relationships between *Pd3* and $R\ (=PGV_{p^*}/PGV_{50\%})$ for probabilities of exceedance at 0.1%, 1%, 5%, and 10%. It shows that when *Pd3* is 0.001 cm the corresponding *R* is highest. The ratio of$R_{max}-R_{min}/R_{max}$ was found to be less than 1.5%.

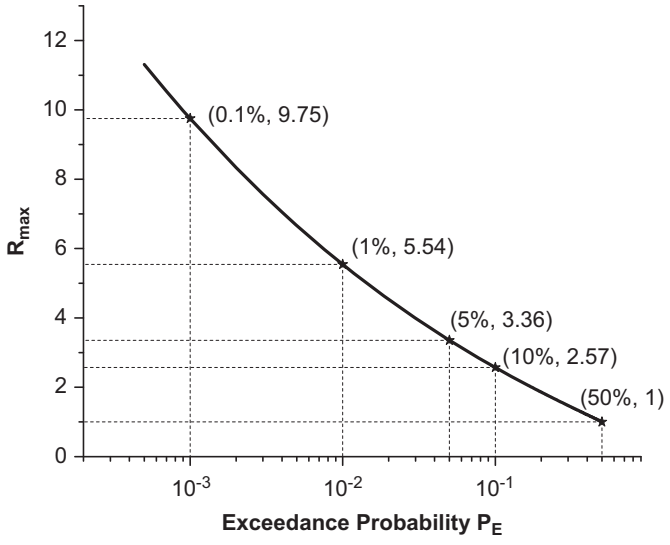

Fig. 6. Relationship between R_{max} and exceedance probability. When exceedance probabilities are 0.1%, 1%, 5%, 10%, and 50%, the respective R_{max} are 9.75, 5.54, 3.36, 2.57, and 1.0.

7. Risk-based decision-making model

It has shown that a *PGV* forecast may vary from the actual observation due to the unavoidable uncertainty in an onsite warning system. In general, larger forecasts are conservative, and are associated with a lower exceedance probability. For the critical design condition where the *PGV* forecast is equal to the design *PGV* of the structure, the failure probability (P_F) equates to the exceedance probability (P_E) of the forecast. This relationship, P_E equal to P_F, assumes a deterministic criterion with global failure when the design *PGV* is exceeded. This consequence from this type of failure can be severe, including loss of life (*LOL*) either from the direct collapse of the structure or from the panicked response of the people after the warning alert is received [16].

This section suggests a risk-based model for deciding whether or not to transmit a warning, with the intention to minimize *LOL* by considering the factors such as the uncertainty of the early warning system, the magnitude of precursor, and the characteristic of warning recipients. The people potentially endangered by an event, such as building occupants during a building collapse, are considered the population at risk (*PAR*). When the earthquake ground motion is equal to or greater than the design *PGV* of a building, *LOL* resulting from the building collapse is as follows:

$$LOL = PAR \times P_F \times p_k \tag{7}$$

where p_k denotes the casualty ratio among *PAR*, with 1.0 being the worst possible scenario. For a global failure the *PGV* forecast is equal to or greater than the design *PGV*, so the P_F associated with an observed precursor (*Pd3*) can be derived from Eq. (4)

$$\begin{aligned} P_E(y^*|x^*) = P_E(y_d|x^*) &= \mathbf{P}(Y > y_d|x^*) \\ &= 1-\mathbf{P}(Y \le y_d|x^*) \\ &= 1-F_{T,n-2}\left(\frac{y_d-\hat{y}_{x^*}}{S_{x^*}}\right) \\ &= P_F(y_d|x^*) \end{aligned} \tag{8}$$

where y_d denotes the logarithm of design *PGV* and x^* denotes an observed log(*Pd3*). Large magnitude precursors lead to the increase P_F, since the design *PGV* is a constant, as shown in

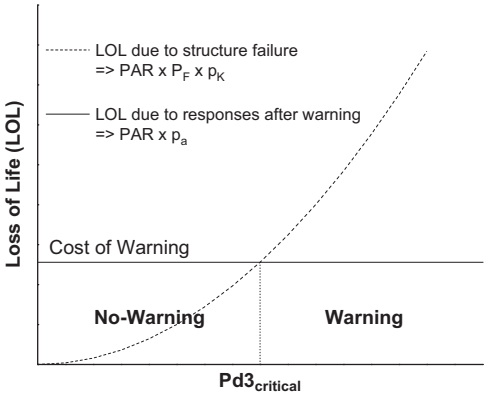

Fig. 7. Decision-making rule for the onsite early warning system. The *LOL* resulting from building collapse is conditional to an observed precursor, but the other one resulting from the post-warning responses is independent of the precursor. When a *Pd3* exceeds the critical value, the decision of issue-warning is needed.

Fig. 3. Similarly, *LOL* resulting from a building collapse will increase proportionally with the value of the observed precursor.

On the other hand, false warnings – building collapse does not occur provided a warning is issued – also have the potential to result in *LOL*. Eq. (9) describes the potential *LOL* after a warning, but when the building is not subject to complete failure.

$$LOL = PAR \times p_a \tag{9}$$

where p_a denotes the casualty ratio among *PAR* after a warning for an event that does not results in complete failure. In this case, *LOL* is independent of the precursor *Pd3*. To minimize *LOL* the decision-making rule becomes

$$D{-}M = \begin{cases} \text{Issue warning} & P_F \times p_k > p_a \\ \text{No warning} & \text{otherwise} \end{cases} \tag{10}$$

Fig. 7 shows a systematic diagram illustrating the decision-making rule. The *LOL* resulting from building collapse begins to exceed the warning without collapse scenario when the observed *Pd3* exceeds a critical value. At that critical value the warning decision should be made. A building with a low P_F (solid design), low p_k and high p_a has a high critical value of *Pd3*.

The cost associated with issuing a warning decision without a building collapse is equal to a $LOL = PAR \times p_a$ (Eq. (9)). The negative consequence of this decision must be surpassed by the savings associated by a successful warning. This concept is analogs to insurance, where $PAR \times p_a$ is the cost of the premium. When the observed precursor is less than the critical value, the insurance is not worth the cost.

8. Discussion

The risk-based model helps to decide whether or not a warning is needed considering factors, such as the magnitude of the observed precursors, the uncertainty of early warning modeling, and the characteristics of warning recipients. A deterministic approach, while not perfect, was adopted in this study for the model development. The model can be extended and improved by adopting a probabilistic failure criterion and considering *PAR* and casualty ratios as random variables. For instance, the *PAR* and p_a associated with most buildings should be time-dependent. The decision-making rule could be further modified to incorporate the time-dependency of these variables.

When a probabilistic criterion in structural failure is adopted, the failure probability becomes a function of the design variables. Considering the structural safety is typically governed by the single design parameter of *PGV*, the resulting structural failure probability P_{SF} (no longer 0 or 1) corresponds to a specific *PGV*. Coupled with the onsite early warning system, the resultant structural failure probability is the product of the exceedance probability (P_E) of a *PGV* forecast, and the structural failure probability (P_{SF}) for the given forecast. Using the probabilistic criterion for the structural failure, *LOL* resulting from the building collapse becomes $LOL = PAR \times P_E \times P_{SF} \times p_k$. When the probabilistic failure criterion becomes associated with multiple design variables, analytical complexity and computational effort is increased. While the inclusion of additional variables may extend the decision-making model by making it more robust, the added complexity also has the negative consequence of making the model computation more expensive and time consuming, delaying the warning notification. The complexity of the decision-making model cannot be extended without limit, since time is the most essential factor in any earthquake earning warning system.

9. Conclusions

This study examined the inherent uncertainty of a specific onsite earthquake early warning developed by using seismic data from Taiwan, Japan and South California. The onsite system takes advantage of the strong correlation between *Pd3* and *PGV*. Since the uncertainty is unavoidable in the onsite system, the *PGV* forecast can be made in a deterministic manner with the forecast for *PGV* equal to $32.98 \times Pd3^{0.81}$. This relationship will result in a 50% probability that the forecast will be exceeded by the actual observation.

This study applies a statistical procedure to estimate *PGV* for a given precursor and exceedance probability. An approximate, but conservative, *PGV* can be conveniently estimated by the proposed generalized relationship, which involves the scaling of the precursor measurement. As an example, the scaling factor of 3.33 is associated with the exceedance probability equal to 5%, resulting in a generalized *PGV* forecast of $110.8 \times Pd3^{0.81}$.

To complement the early earthquake warning system, a risk-based, decision-making model was also proposed to aid in the decision of whether or not a warning is needed for an observed precursor. The decision-making rule is intended to minimize the loss of life from the resulting events.

Acknowledgments

The authors thank Dr. Su-Chin Chang of the University of Hong Kong, and Dr. Yeou-Koung Tung of the Hong Kong University of Science and Technology for their constructive comments during the development of this paper. We also appreciate the valuable comments from the anonymous reviewers.

Appendix I [17]

The variance of prediction error $V[Y-(\hat{\beta}_0+\hat{\beta}_1 x^*)]$ is

$$\begin{aligned} V\left[Y-(\hat{\beta}_0+\hat{\beta}_1 x^*)\right] &= V(Y)+V(\hat{\beta}_0+\hat{\beta}_1 x^*) \\ &= s^2+s^2\left[\frac{1}{n}+\frac{(x^*-\bar{x})^2}{S_{xx}}\right] \\ &= s^2\left[1+\frac{1}{n}+\frac{(x^*-\bar{x})^2}{S_{xx}}\right] = {S_{x^*}}^2 \end{aligned} \tag{I.1}$$

where s is the standard deviation of the regression model, n is the sample size, $\hat{\beta}_0$, $\hat{\beta}_1$ are the point estimates of model parameters,

and x^* denotes an observation of the independent variable X. The sum of square of X, S_{xx}, is defined as follows:

$$S_{xx} = \sum_{i=1}^{n} (x_i - \bar{x})^2 \tag{I.2}$$

The expectation of prediction error is

$$E[Y-(\hat{\beta}_0+\hat{\beta}_1 x^*)] = E(Y)-\hat{\beta}_0+\hat{\beta}_1 x^* = 0 \tag{I.3}$$

Since the prediction error follows a t-distribution, combining Eqs. (I.1) and (I.2) gives a random variable T following the t-distribution with $n-2$ degree of freedom

$$T = \frac{Y-(\hat{\beta}_0+\hat{\beta}_1 x^*)-E[Y-(\hat{\beta}_0+\hat{\beta}_1 x^*)]}{\sqrt{V[Y-(\hat{\beta}_0+\hat{\beta}_1 x^*)]}} = \frac{Y-(\hat{\beta}_0+\hat{\beta}_1 x^*)}{s\sqrt{\left[1+\frac{1}{n}+\frac{(x^*-\bar{x})^2}{S_{xx}}\right]}} \tag{I.4}$$

Appendix II

A forecast Y at a given exceedance probability p^* and an observed x^*:

From Eq. (4),

$$\begin{aligned} 1-\mathbf{P}(P_E = p^*, X = x^*) &= F_{T,n-2}\left(\frac{Y_{p^*,x^*}-\hat{y}_{x^*}}{S_{x^*}}\right) \\ &= > \frac{Y_{p^*,x^*}-\hat{y}_{x^*}}{S_{x^*}} = F^{-1}_{T,n-2}\{1-\mathbf{P}(P_E = p^*, X = x^*)\} \\ &= > Y_{p^*,x^*} = F^{-1}_{T,n-2}\{1-\mathbf{P}(P_E = p^*, X = x^*)\}S_{x^*}+\hat{y}_{x^*} \end{aligned} \tag{II.1}$$

where $S_x{}^*$ is shown in Eq. (I.1); $F_{T,n-2}$ and $F^{-1}_{T,n-2}$ denote the cumulative probability function and inversed probability function of a t variate with n–2 degree of freedom, respectively.

References

[1] Wu YM, Kanamori H. Development of an earthquake early warning system using real-time strong motion signals. Sensors 2008;8:1–9.

[2] Nakamura Y. Development of the earthquake early warning system for the Shinkansen, some recent earthquake engineering research and practical in Japan. The Japanese National Committee of the International Association for Earthquake Engineering 1984:224–38.

[3] Allen RM, Kanamori H. The potential for earthquake early warning in Southern California. Science 2003;300:786–9.

[4] Horiuchi S, Negishi H, Abe K, Kamimura A, Fujinawa Y. An automatic processing system for broadcasting earthquake alarms. Bulltin of the Seismological Society of America 2005;95:708–18.

[5] Wu YM, Kanamori H. Experiment on an onsite early warning method for the Taiwan early system. Bulletin of the Seismological Socety of America 2005; 95:347–53.

[6] Wu YM, Kanamori H. Rapid assessment of damaging potential of earthquakes in Taiwan from the beginning of P waves. Bulletin of the Seismological Society of America 2005;95:1181–5.

[7] Wu YM, Kanamori H. Exploring the feasibility of on-site earthquake early warning using close-in records of the 2007 Noto Hanto earthquake. Earth Planets and Space 2008;60:155–60.

[8] Wu YM, Kanamori H, Allen RM, Hauksson E. Determination of earthquake early warning Parameters, τc and Pd, for southern California. Geohpysical Journal International 2007;170:711–7.

[9] Kanamori H, Hauksson E, Heaton T. Real-time seismology and earthquake hazard mitigation. Nature 1997;390:461–4.

[10] Kanamori H. Real-time seismology and earthquake damage mitigation. Annual Review of Earth and Planetary Sciences 2005;33:195–214.

[11] Iervolino I, Convertito V, Giorgio M, Manfredi G, Zollo A. Real-time risk analysis for hybrid earthquake early warning systems. Journal of Earthquake Engineering 2006;10:867–85.

[12] Iervolino I, Giorgio MC, Manfredi G. Expected loss-based alarm threshold set for earthquake early warning systems. Earthquake Engineering and Structural Dynamics 2007;36:1151–68.

[13] Iervolino I, Giorgio M, Galasso C, Manfredi G. Uncertainty in early warning predictions of engineering ground motion parameters: what really matters? Geophysical Research Letters 2009;36:1–6.

[14] Iervolino I. Performance-based earthquake early warning. Soil dynamics and Earthquake Engineering 2010. doi:10.1016/j.soildyn.2010.07.010.

[15] Convertito V, Iervolino I, Zollo A, Manfredi G. Prediction of response spectra via real-time earthquake measurements. Soil Dynamics and Earthquake Engineering 2008;28:492–505.

[16] Mileti SM, Peek L. The social psychology of public response to warnings of a nuclear power plant accident. Journal of Hazardous Materials 2000;75: 181–94.

[17] Devore JL. Probability and statistics for engineering and the science, 7th ed. p. 477–82, 501–5, ISBN-10: 0-495-38223-X.